*Supplements to:*

# A System Dynamics Model to Facilitate the Development of Policy for Urban Heat Island Mitigation

---

**Supplement A: Inventory of Data Input Requirements of *UHIMPT* Model**

| Components | Requirement | Potential Sources |
|---|---|---|
| Urban Heat Island, Climate Change Impacts | Normal mean warmest month ambient temperature in the urban area | Climate models; Raster-based geospatial datasets (e.g., Wang et al. [56]) |
| Urban Heat Island, Climate Change Impacts | Normal mean warmest month ambient temperature in the rural area | Climate models; Raster-based geospatial datasets (e.g., Wang et al. [56]) |
| Urban Heat Island, Climate Change Impacts | Normal mean maximum warmest month ambient temperature in the urban area | Climate models; Raster-based geospatial datasets (e.g., Wang et al. [56]) |
| Urban Heat Island, Climate change Impacts | Normal mean maximum warmest month ambient temperature in the rural area | Climate models; Raster-based geospatial datasets (e.g., Wang et al. [56]) |
| Urban Heat Island | Moderate- to high-resolution cloud-free, daytime satellite imagery with ultra-blue, green, red, near infrared, and thermal infrared bands | Landsat 8 may be accessed through the EarthExplorer Internet-based application of the United States Geological Survey |
| Urban Heat Island | Vector-based geospatial dataset representing impervious cover in urban area | Public geospatial data clearinghouses, private organizations |
| Climate Change Impacts | Projected mean warmest month ambient temperature for three periods, as downscaled to the urban area | Climate models; Raster-based geospatial datasets (e.g., Wang et al. [56]) |
| Climate Change Impacts | Projected mean maximum warmest month ambient temperature for three periods, as downscaled to the urban area | Climate models; Raster-based geospatial datasets (e.g., Wang et al. [56]) |
| Climate Change Impacts | Projected mean warmest month ambient temperature for three periods, as downscaled to the rural area | Climate models; Raster-based geospatial datasets (e.g., Wang et al. [56]) |

**Supplement A: Inventory of Data Input Requirements of *UHIMPT* Model (Continued)**

| Components | Requirement | Potential Sources |
|---|---|---|
| Climate Change Impacts | Projected mean maximum warmest month ambient temperature for three periods, as downscaled to the rural area | Climate models; Raster-based geospatial datasets (e.g., Wang et al. [56]) |
| Population Dynamics | Population by single year of birth for last official census | Official census agencies (e.g., United States Census Bureau, Statistics Canada) |
| Population Dynamics | Population by single year of birth for penultimate official census | Official census agencies (e.g., United States Census Bureau, Statistics Canada) |
| Population Dynamics | Total births between last and penultimate census by single year of age of the parous female | Local or regional health departments, offices of vital statistics |
| Population Dynamics | Total deaths between last and penultimate census by single year of age of the decedent | Local or regional health departments, offices of vital statistics |
| Heat-Related Mortality | Normal mean summer ambient temperature in the region | Climate models; Raster-based geospatial datasets (e.g., Wang et al. [56]) |
| Heat-Related Mortality | Normal mean winter ambient temperature in the region | Climate models; Raster-based geospatial datasets (e.g., Wang et al. [56]) |
| Heat-Related Mortality | Projected annual mean ambient temperature for three periods, as downscaled to the region | Climate models; Raster-based geospatial datasets (e.g., Wang et al. [56]) |
| Heat-Related Mortality | Normal annual mean ambient temperature in the region | Climate models; Raster-based geospatial datasets (e.g., Wang et al. [56]) |
| Not Applicable (General Use) | Vector-based geospatial datasets representing the boundaries of the urban and rural areas (n.b., this is used to process raster-based geospatial datasets) | Public geospatial data clearinghouses, private organizations |

**Supplement B: Development of Multiple Linear Regression Model Used in Equations 5 and 6**

**Introduction**

Equations 5 and 6 contain an adaptation of a multiple linear regression model (MLR Model) wherein: the land surface temperature of a given area is the dependent variable; and, the surface albedo and the proportions of impervious surface cover and vegetation in the same area are the independent variables.

The MLR Model is developed with: data derived from a moderate- to high-resolution cloud-free, daytime satellite image; and, digital geographic data on impervious surface cover, land cover, and building footprints in shapefile data format.

The means by which the satellite image and other digital geographic data were processed, as well as how the MLR Model was created, are described in the remainder of this appendix.

Please note that while the MLR Model has been created with data that represents Philadelphia, Pennsylvania, this location only serves as an illustrative example. The methodologies explained herein are easily replicated, and similar MLR Models can be developed for customization of the *UHIMPT* model to other locations.

**Image Processing**

Moderate- to high-resolution satellite imagery is processed to extract data for entry into the MLR Model. In this example, a Landsat 8 Operational Land Imager/Thermal Infrared Sensor Tier 1 image was downloaded from the EarthExplorer Internet application of the United States Geological Survey, which is located at http://earthexplorer.usgs.gov, on 22 October 2017 and subsequently processed to retrieve information on the aforementioned dependent variable and independent variables. The image was captured by the Landsat 8 spacecraft on 30 July 2017 at approximately 15:39. The United States Geological Survey's unique identification number of this image is "LC80140322017211LGN00". The image includes essentially cloud-free coverage of Philadelphia and surrounding areas and represents warmest month conditions. It was processed with ArcGIS Desktop (Release 10.5.1) geographic information system software by ESRI, Inc. of Redlands, California. The image's pixel dimension is 30 m by 30 m for bands captured by the Operational Land Imager.

**Supplement B: Development of Multiple Linear Regression Model Used in Equations 5 and 6 (Continued)**

For bands captured by the Thermal Infrared Sensor, the pixel dimension is 100 m by 100 m. However, bands captured by the Thermal Infrared Sensor are resampled to 30 m prior to distribution.

The following subsections provide details on data derivation from the aforementioned Landsat 8 Operational Land Imager/Thermal Infrared Sensor Tier 1 image. Please note that the methodologies presented herein are applicable to other satellite products, should another source of satellite imagery be used.

**Derivation of Proportion of Vegetation**

Deriving proportion of vegetation is a two-step process. First, the Normalized Difference Vegetation Index (NDVI), is calculated with the near-infrared and red bands of the aforementioned image by means of the NDVI function of ArcGIS Desktop. NDVI is used to assess whether an area contains living green vegetation and quantify same relative to other areas. It was first mentioned by Rouse et al. [75] and is calculated as:

$$NDVI = \frac{NIR - R}{NIR + R},$$

where: $NDVI$ means Normal Difference Vegetation Index; $NIR$ represents the near-infrared band of the image (viz., Band 5); and, $R$ represents the red band of the image (viz., Band 4). Once calculated, NDVI is transformed into proportion of vegetation by means for the following formula, which is provided in Jiménez-Muñoz et al. [76] as:

$$P_v = \left(\frac{NDVI - NDVI_s}{NDVI_v - NDVI_s}\right)^2,$$

where: $P_v$ stands for the proportion of vegetation; and, the subscripts of $NDVI$ stand for the maximum $(v)$ and minimum $(s)$ of same.

The application of the formula provided above yields an accessible measure of the amount of vegetation in each pixel, which ranges from 0.0 to 1.0, with 0.0 representing no vegetation and 1.0 representing complete vegetative cover.

**Supplement B: Development of Multiple Linear Regression Model Used in Equations 5 and 6 (Continued)**

**Derivation of Land Surface Temperature**

Land surface temperature is calculated with the proportion of vegetation ($P_v$), and is entered into the MLR Model as the averaged values of both thermal infrared bands of the image (viz., Band 10 and Band 11). The employed methodology is generally described in Avdan and Jovanovska [77]. Please note, however, that slight modifications are made to apply: a more recent formula by the United States Geological Survey [78] for the calculation of spectral radiance; and, a simplified (i.e., average) calculation of land surface emissivity by Sobrino et al. [79].

The first step is to calculate spectral radiance at the top of the atmosphere as in the following formula by the United States Geological Survey [78]:

$$L_\lambda = (M_L \times Q_{Cal}) + A_L,$$

where: $L_\lambda$ represents the spectral radiance at the top of the atmosphere; $M_L$ is the band-specific multiplicative rescaling factor that is provided in the image's metadata; $Q_{Cal}$ is the pixel value; and, $A_L$ is the band-specific additive rescaling factor that is provided in the image's metadata.

The second step is to calculate at-satellite brightness temperature as in the following formula by the United States Geological Survey [78] and modified by Avdan and Jovanovska [77] to convert from °K to °C:

$$SBT = \left(\frac{K_2}{\ln\left(\frac{K_1}{L_\lambda} + 1\right)}\right) - 273.15,$$

where: $SBT$ represents at-satellite brightness temperature; $L_\lambda$ represents the spectral radiance at the top of the atmosphere, which has been explained above; and, $K_1$ and $K_2$ represent the band-specific thermal conversion constants that are provided in the image's metadata.

The third step is to calculate land surface emissivity, for which the following formula by Sobrino et al. [79] is applied:

$$\varepsilon = (0.004 \times P_v) + 0.986,$$

where $\varepsilon$ is land surface emissivity and $P_v$ is the proportion of vegetation, both as previously discussed in this appendix.

**Supplement B: Development of Multiple Linear Regression Model Used in Equations 5 and 6 (Continued)**

The fourth step is to separately calculate the land surface temperature for both thermal infrared bands (viz., Band 10 and Band 11) of the image as in the following formula by Avdan and Jovanovska [77]:

$$LST = \frac{SBT}{\left(1 + \left(\left(\frac{\lambda \times SBT}{\rho}\right) \ln \varepsilon\right)\right)},$$

where: $LST$ represents land surface temperature; $SBT$ represents at-satellite brightness temperature, which has been previously discussed in this appendix; $\varepsilon$ represents land surface emissivity; $\lambda$ represents the wavelength of emitted radiance, which is assumed to be 10.896 and 12.006 for Band 10 and Band 11, respectively (Yu et al. [80]); and, $\rho$ is equivalent to $1.438 \times 10^{-2}\ mK$, as calculated by the following formula:

$$\rho = h\frac{c}{\sigma} = 1.438 \times 10^{-2}\ mK,$$

where: $h$ is Plank's constant ($6.626 \times 10^{-34}\ J/s$); $\sigma$ is the Boltzmann constant ($1.38 \times 10^{-23}\ J/K$); and, $c$ is the velocity of light ($2.998 \times 10^{8}\ m/s$).

The fifth and final step is to compute the average land surface temperature for both thermal infrared bands (viz., Band 10 and Band 11). This is the measure of land surface temperature that is entered into the MLR Model. The average land surface temperature for both thermal infrared bands is computed as follows:

$$LST_{Entered} = \frac{(LST_{Band\ 10} + LST_{Band\ 11})}{2},$$

where: $LST_{Entered}$ represents the measure of land surface temperature that is entered into the MLR Model; $LST_{Band\ 10}$ is the land surface temperature reflected in Band 10, as computed in the fourth step; and, $LST_{Band\ 11}$ is the land surface temperature reflected in Band 11, also as computed in the fourth step.

Please note that land surface temperature is calculated in °C.

**Surface Albedo**

The following formula of Lee et al. [81] is used to calculate surface albedo:

$$A = 0.166_{Band_2} + 0.321_{Band_4} + 0.355_{Band_5} - 0.027_{Band_6} + 0.150_{Band_7} - 0.0037,$$

where: $A$ represents albedo; and, the subscripts denote band numbers of the image.

**Supplement B: Development of Multiple Linear Regression Model Used in Equations 5 and 6 (Continued)**

Surface albedo ranges from 0.0 to 1.0, with 0.0 representing no reflectivity and 1.0 representing total reflectivity.

Please note that, in this example, surface albedo was calculated from a version of the aforementioned Landsat 8 Operational Land Imager/Thermal Infrared Sensor Tier 1 image that was specially processed by the United States Geological Survey to provide surface reflectance data. This version of the image was ordered through the Earth Science Processing Architecture On-Demand Interface of the Earth Resources Observation and Science Center of the United States Geological Survey on 30 October 2017. The Earth Science Processing Architecture On-Demand Interface is located at https://espa.cr.usgs.gov/.

**Water Features**

Although not used as an independent variable in the MLR Model that is represented in equations 5 and 6, the Modified Normalized Difference Water Index (MNDWI), as is described by Xu [82], is calculated to facilitate the identification of water features so that they may be excluded from the input of the MLR Model.

The complete exclusion of water features is important because they have the potential to skew the results of the MLR Model. Indeed, water features tend to have both low surface albedos and low surface temperatures. This is generally the inverse of the relationship between surface albedo and surface temperature over land, where low albedo surfaces would be expected to have a high surface temperature.

The following formula of Xu [82] is used to calculate MNDWI:

$$MNDWI = \frac{G - MIR}{G + MIR},$$

where: $MNDWI$ is the Modified Normalized Difference Water Index; $G$ represents the green band of the image; and, $MIR$ represents the middle infrared band of the image.

As has been previously stated, MNDWI is used to facilitate feature identification and extraction. In this regard, it is noted that positive MNDWI values represent water and negative values represent land. However, once calculated, MNDWI must subsequently be compared against the image in order to ensure the appropriateness of feature extraction. The reason for this is that MNDWI can be prone to errors resulting from shadows and atmospheric conditions reflected in the image, which, may cause

some areas to have a positive value when, in fact, they are not covered by water and should, therefore, not be extracted.

In addition to a visual comparison of calculated MNDWI and the image, other available resources should also be used to ensure that water features are accurately selected and excluded. In this example, a digital geographic dataset on land cover in Philadelphia, which was created by the City of Philadelphia in 2016 and obtained from the Internet site of the Pennsylvania Geospatial Data Clearinghouse at http://www.pasda.psu.edu/uci/DataSummary.aspx?dataset=7046 on 30 September 2017, was used to identify additional pixels for exclusion by means of the locational selection functions of ArcGIS Desktop.

Only the data of pixels that are located completely outside of a water feature are entered into the MLR Model.

**Impervious Surface Data Processing**

The calculated proportion of impervious surface cover is also entered into the MLR Model.

In this example, digital geographic data on impervious surface cover and building footprints in Philadelphia was obtained from the Internet site of the Pennsylvania Geospatial Data Clearinghouse. Specifically, the following data was obtained: a shapefile depicting impervious surface cover during Spring 2015, which was created by the City of Philadelphia and downloaded from http://www.pasda.psu.edu/uci/FullMetadataDisplay.aspx?file=PhiladelphiaImperviousSurfaces2015.xml on 30 September 2017; and, a shapefile depicting building footprints during 2015, which was created by the City of Philadelphia and downloaded from http://www.pasda.psu.edu/uci/DataSummary.aspx?dataset=146 on 30 September 2017.

The aforementioned data layers were processed by first merging and then dissolving them with the corresponding geoprocessing functions of ArcGIS Desktop. This resulted in one data layer with a single feature, which depicted all impervious surfaces within Philadelphia; this data layer is hereinafter referred to as the interim impervious surface layer.

Next, interim impervious surface layer was intersected, by means of the corresponding geoprocessing function of ArcGIS Desktop, with a vector-based fishnet grid to make it (i.e., the interim impervious surface layer) gridded. The boundaries and number of features in the vector-based fishnet grid

mimicked those of the pixels of the aforementioned satellite image. This grid was created by: first converting a copy of the satellite-derived, raster-based information on land surface temperature, which was previously introduced in this appendix, to point features by means of the Raster to Point function of ArcGIS Desktop; and, then using the resulting point-based data layer to create a grid by means of the "Create Fishnet" function of ArcGIS Desktop with the individual cell size being set to 30 m in height and 30 m in width.

After intersecting the interim impervious surface layer with the vector-based fishnet grid, the area of impervious surface cover, as measured in square meters (i.e., $m^2$), within each cell was computed. The intersected impervious surface layer was then dissolved, by means of the corresponding geoprocessing function of ArcGIS Desktop. While doing so, the unique cell identifier was retained, and the total impervious surface cover in each unique cell was summed. At this point, a new field was created in the attribute table, and the proportion of total impervious surface cover in each unique cell was computed by means of the following formula:

$$P_i = \frac{\sum i}{900},$$

where $P_i$ represents proportion of impervious surface cover and $i$ represents impervious cover. The divisor (900) represents the total area of each unique cell (n.b., $30^2 = 900$). All measurements are made in square meters (i.e., $m^2$).

The final result of these operations was a data layer showing the proportion of impervious surface cover in cells that matched the pixel dimensions and arrangement of the satellite-derived information that has been previously discussed in this appendix.

Please note that impervious surface cover is measured on a scale of 0.0 to 1.0, with 0.0 representing no impervious surface cover and 1.0 representing total impervious surface cover.

**Data Processing Results**

Images showing proportion of vegetation, land surface temperature, surface albedo, water features, and impervious surface cover in Philadelphia are provided on the following pages. Please note that water features have not been removed from the images of proportion of vegetation, land surface temperature, surface albedo, and impervious surface cover.

**Supplement B: Development of Multiple Linear Regression Model Used in Equations 5 and 6 (Continued)**

*Proportion of Vegetation*

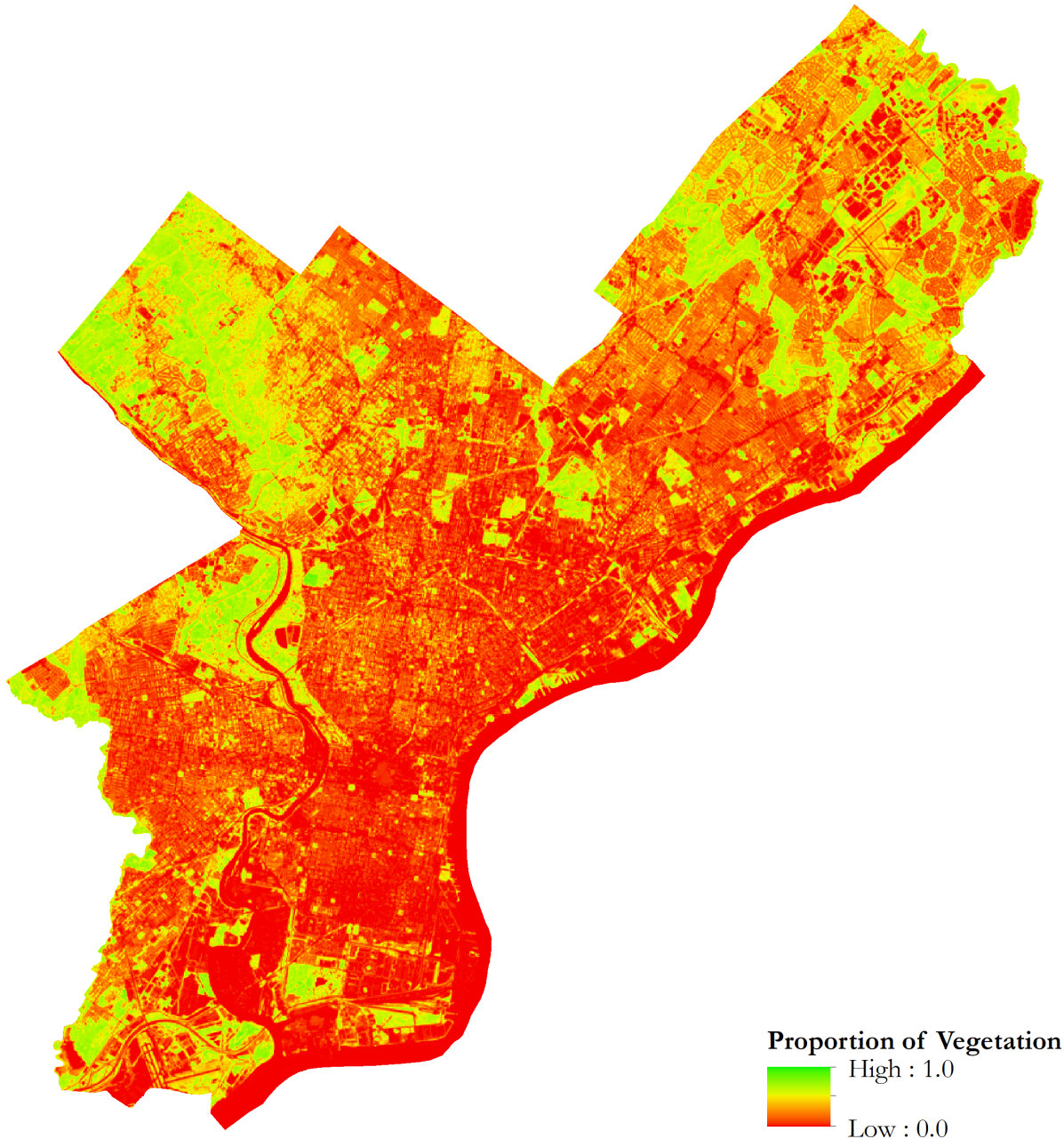

**Supplement B: Development of Multiple Linear Regression Model Used in Equations 5 and 6 (Continued)**

*Surface Temperature*

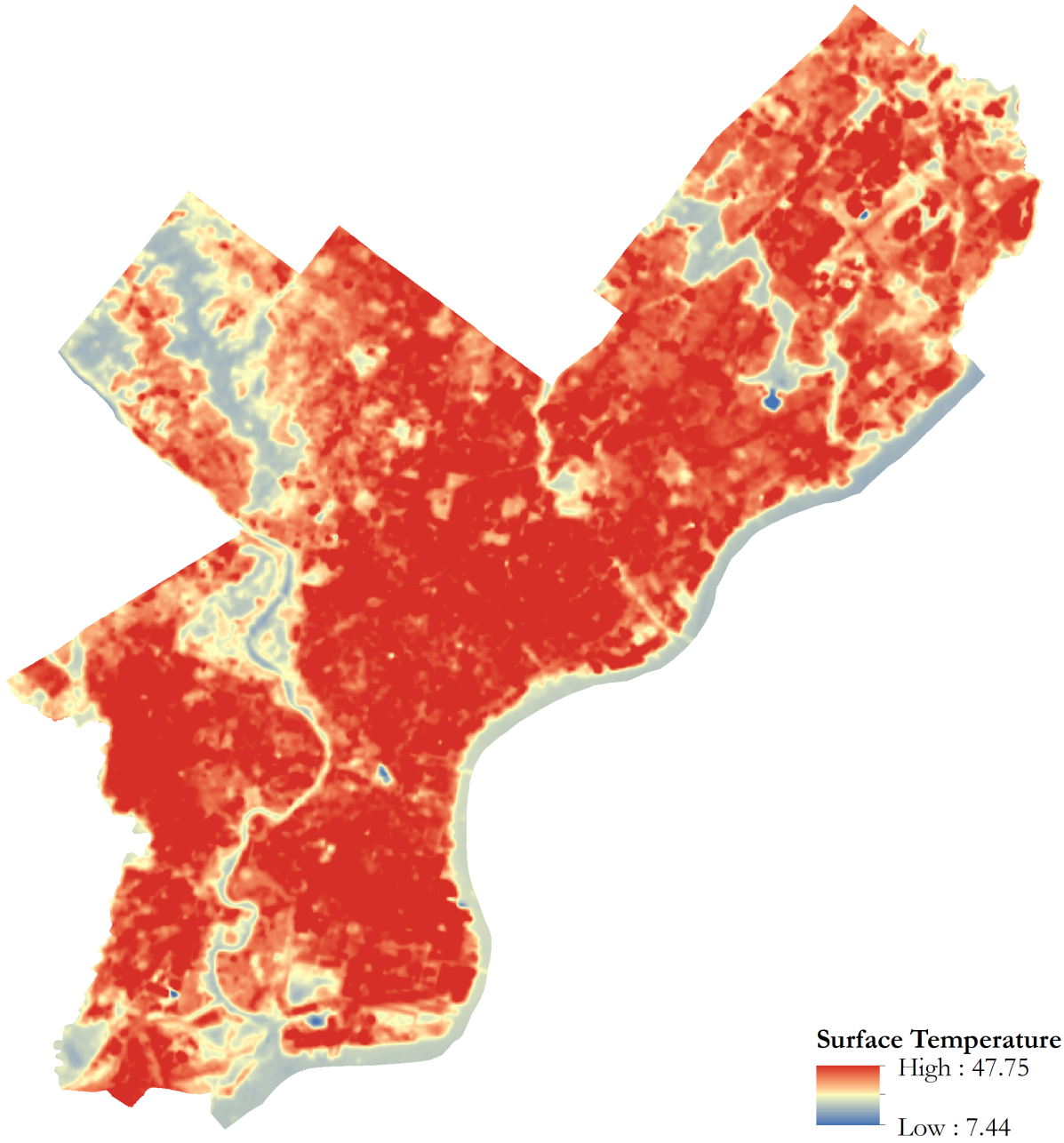

**Supplement B: Development of Multiple Linear Regression Model Used in Equations 5 and 6 (Continued)**

*Surface Albedo*

**Supplement B: Development of Multiple Linear Regression Model Used in Equations 5 and 6 (Continued)**

*Water Features (MNDWI)*

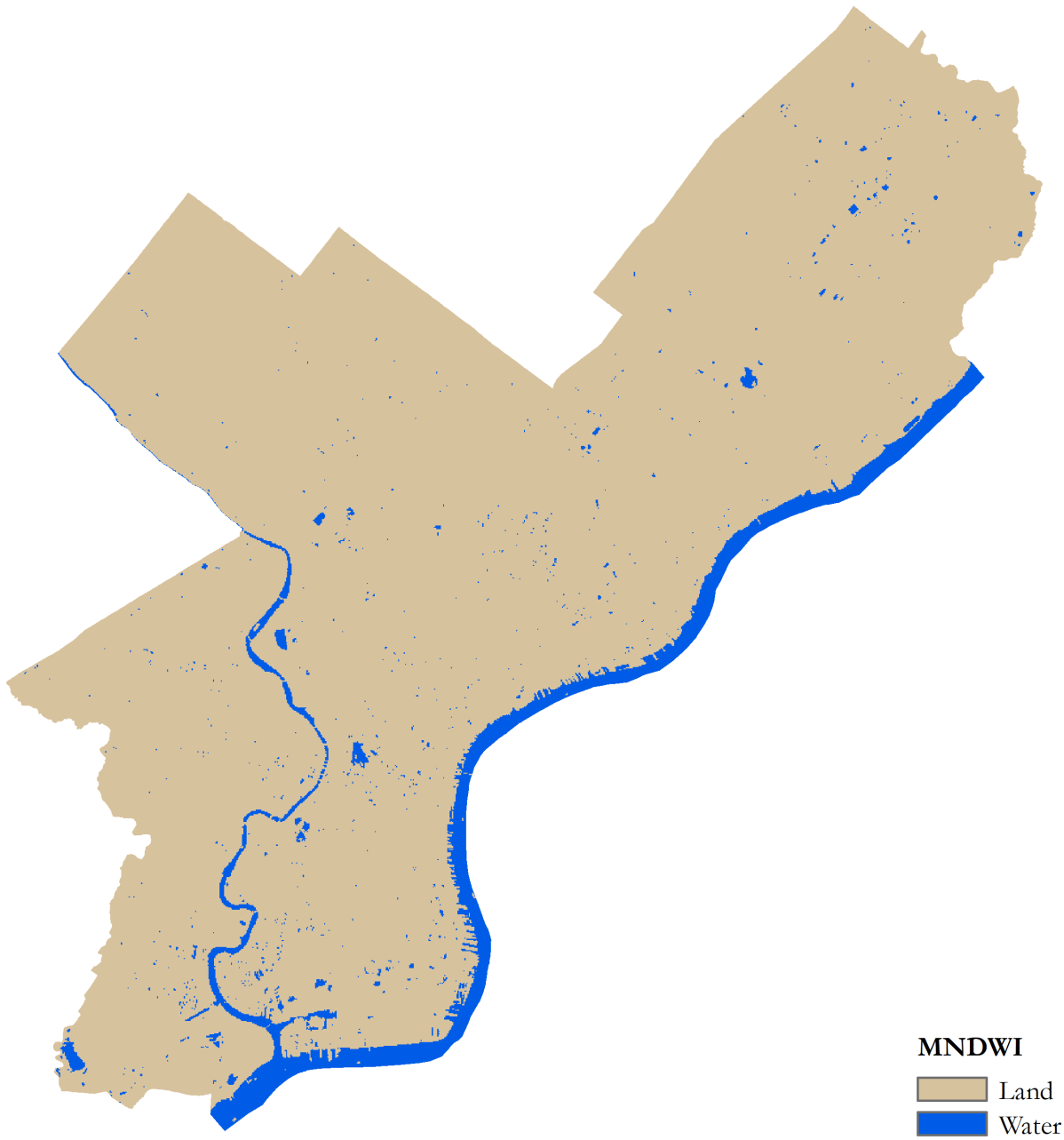

**Supplement B: Development of Multiple Linear Regression Model Used in Equations 5 and 6 (Continued)**

*Impervious Surface Cover*

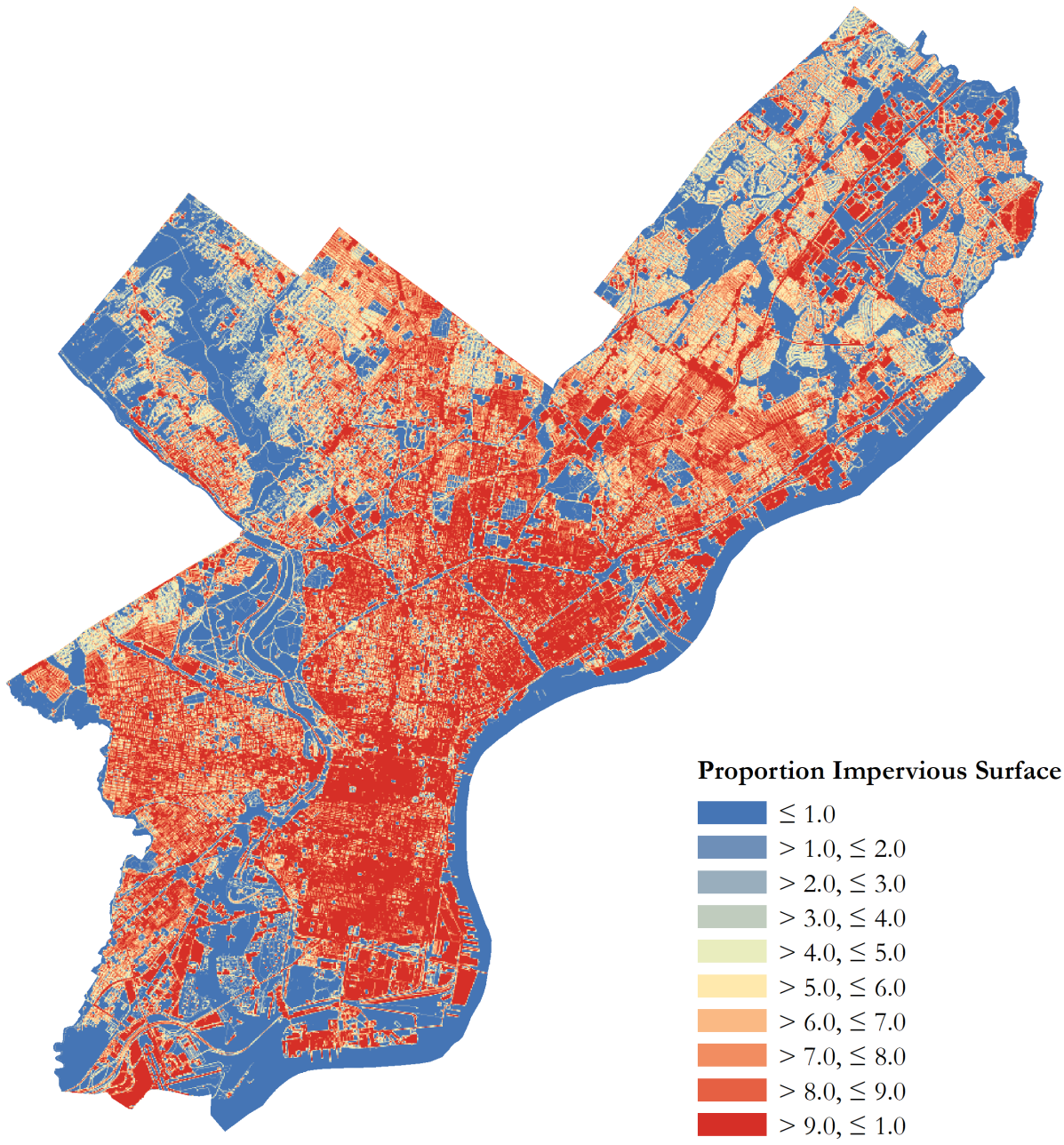

**Supplement B: Development of Multiple Linear Regression Model Used in Equations 5 and 6 (Continued)**

**Development of Multiple Linear Regression (MLR) Model**

At the outset of the development of the MLR Model, the satellite-derived data on proportion of vegetation, land surface temperature, and surface albedo, as well as the processed, vector-based data on impervious surface cover, were combined into one data layer. This was achieved by first converting the raster-based (i.e., satellite-derived) data layers (viz., proportion of vegetation, land surface temperature, surface albedo) to vector-based files, and then joining the attribute tables of all converted data layers with that of impervious surface cover. The end result was one composite, vector-based file with a single attribute table that contained complete information on each of the independent and dependent variables. Water features, as identified with the methodologies described herein, were then used to select cells in the composite file that fell wholly or partially within a water feature. The selected cells were deleted from the composite file and excluded from further analysis. As previously noted, this was done to prevent albedo over water surfaces from skewing the MLR Model's depiction of the correlation between land surface temperature and surface albedo (n.b., the albedo and surface temperature of water features is generally low; on land, however, low albedo surfaces are generally associated with high surface temperatures). At this point, the attribute table of the composite file was exported for analysis in IBM SPSS Statistics (Release 25), which is a statistical analysis software package by IBM Corporation of Armonk, New York. There was a total of 379,419 records in the exported data table. Each record depicted average conditions within an area measuring 30 m by 30 m and with a centroid located on land surface within the municipal boundaries of Philadelphia, Pennsylvania.

A stepwise multiple linear regression analysis was then run in IBM SPSS Statistics. All data inputs were derived from the exported attribute table of the composite file. The dependent variable was land surface temperature, and the independent variables were surface albedo, proportion of vegetation, and the proportion of impervious surface cover. The resulting MLR Model indicated that when the impact on land surface temperature is predicted, surface albedo ($N = 379{,}419;\ \beta = -5.874;\ p < .0005;\ 95\text{-}Percent\ CI = -6.042, -5.707$), impervious surface cover ($N = 379{,}419;\ \beta = 2.103;\ p < .0005;\ 95\text{-}Percent\ CI = 2.078, 2.128$), and the proportion of vegetation ($N = 379{,}419;\ \beta = -8.730;\ p < .0005;\ 95\text{-}Percent\ CI = -8.779, -8.681$) are highly significant predictors. The coefficient of multiple determination ($r^2$) of the MLR Model is 0.63.

**Supplement B: Development of Multiple Linear Regression Model Used in Equations 5 and 6 (Continued)**

The MLR Model is summarized by the following formula:

$$LST = 31.661 + (2.103 \times I) - (8.730 \times V) - (5.874 \times A),$$

where: $LST$ represents land surface temperature; $I$ represents the proportion of impervious surface cover; $V$ represents the proportion of vegetation; and, $A$ represents surface albedo.

It should be noted that inclusion of the three independent variables (viz., proportion impervious surface cover, proportion of vegetation, and surface albedo) together resulted in a higher coefficient of multiple determination ($r^2$) than would have been possible if linear regression analysis had been performed in any other possible way, including: simple linear regression of the proportion impervious surface cover, which would have resulted in a coefficient of determination ($r^2$) of 0.50; simple linear regression of the proportion of vegetation, which would have resulted in a coefficient of determination ($r^2$) of 0.59; simple linear regression of surface albedo, which would have resulted in a coefficient of determination ($r^2$) of 0.01; multiple linear regression of the proportions of vegetation and impervious surface cover, which would have resulted in a coefficient of multiple determination ($r^2$) of 0.62; multiple linear regression of surface albedo and the proportion of impervious surface cover, which would have resulted in a coefficient of multiple determination ($r^2$) of 0.51; and, multiple linear regression of surface albedo and the proportion of vegetation, which would have resulted in a coefficient of multiple determination ($r^2$) of 0.60.

It should further be noted that the MLR Model is based on an approximately normally distributed dataset. This is demonstrated by the following histogram of regression standardized residuals.

**Supplement B: Development of Multiple Linear Regression Model Used in Equations 5 and 6 (Continued)**

*Histogram of Regression Standardized Residual*

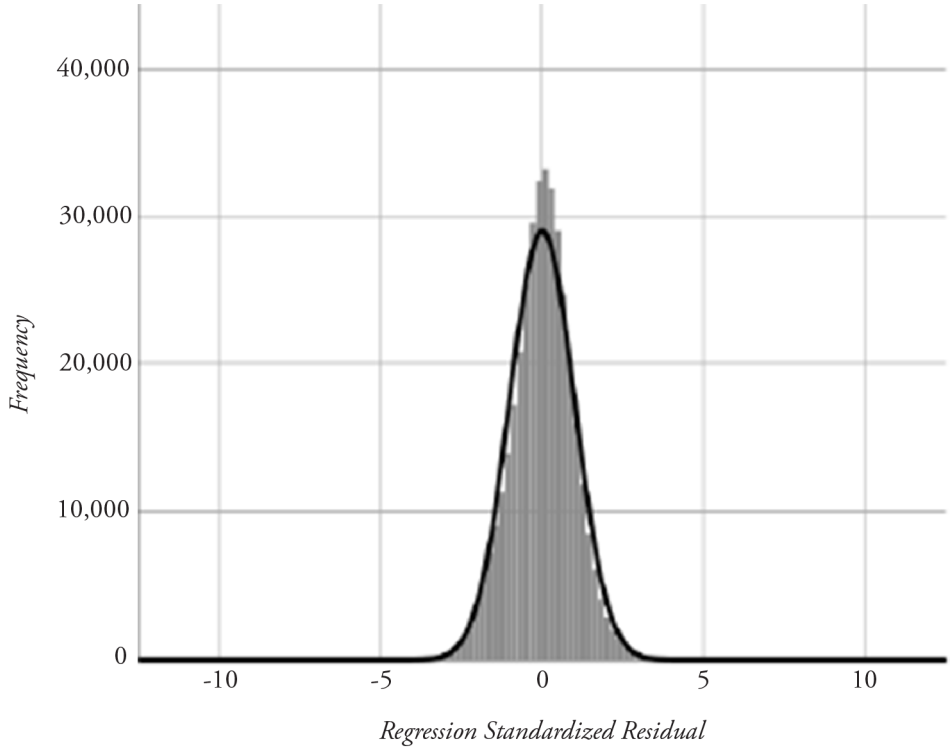


As can be seen in the histogram of regression standardized residuals, the distribution of the dataset is approximately symmetrical and short-tailed. These characteristics suggest a normally distributed dataset.

The normal distribution of the dataset on which the MLR Model is based can also be seen in the following normal probability–probability plot of regression standardized residual.

**Supplement B: Development of Multiple Linear Regression Model Used in Equations 5 and 6 (Continued)**

*Normal Probability–Probability Plot of Regression Standardized Residual*

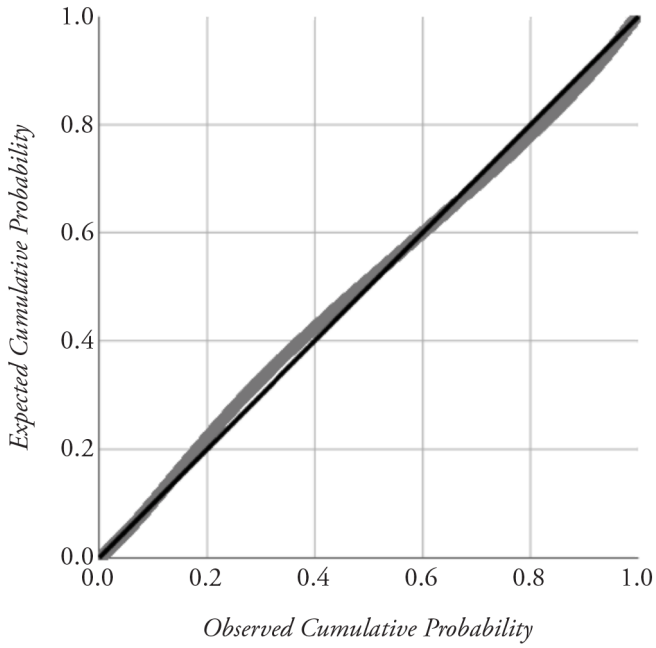


As can be seen in the normal probability–probability plot of regression standardized residuals, there is no skew to the left or right, nor do the extremes of observed cumulative probability show significant departures from expected cumulative probability (i.e., the data do not have long or short tails). In addition, the coefficient of determination ($r^2$) between observed cumulative probability and expected cumulative probability is greater (i.e., >) than 0.99. These characteristics facilitate the conclusion that the dataset is normally distributed.

In addition to the above, it is noted that, because it has been developed with data that represents all areas of land surface within Philadelphia, the MLR Model should be understood to represent the average relationship between the independent variables and the dependent variable. This comports with the intent, purpose and requirements of the *UHIMPT* model, which has been presented in the article. It is, nonetheless, interesting to note that if records for specific subareas of Philadelphia (e.g., wards) were to be selected from the composite file, regression models with a higher coefficient of multiple determination ($r^2$) may be achieved. For example, if the records of the aforementioned composite file that intersect Ward 34, which is located at the westernmost point of Philadelphia, were selected and a multiple linear regression analysis of the selected records were run in the same manner as has been done

**Supplement B: Development of Multiple Linear Regression Model Used in Equations 5 and 6 (Continued)**

for the entirety of Philadelphia, the following model, which achieves a coefficient of multiple determination ($r^2$) of 0.78, would result:

$$LST_{Ward\ 34} = 32.886 + (0.942\ \times\ I_{Ward\ 34}) - (11.326\ \times\ V_{Ward\ 34}) - (2.470\ \times\ A_{Ward\ 34}),$$

where: $LST$ represents land surface temperature; $I$ represents the proportion of impervious surface cover; $V$ represents the proportion of vegetation; $A$ represents surface albedo; and, subscripts specify values for Ward 34.

As noted above, the foregoing model achieves a coefficient of multiple determination ($r^2$) of 0.78. This is 0.15 higher than the model that is applicable to the entirety of Philadelphia (i.e., the MLR Model), which achieved a coefficient of multiple determination ($r^2$) of 0.63. The reason why higher coefficients of multiple determination may be achieved when the data represent a specific subarea of the Philadelphia lies in the fact that the citywide data may, depending upon how data is resampled, include a higher degree of variability. Resampling the data may help to remove a significant degree of this variability, and thereby facilitate the achievement of a higher coefficient of multiple determination ($r^2$). However, because the intent of the *UHIMPT* model was to represent average conditions in order to support citywide analysis, the regression model developed with all 379,419 data points (i.e., the MLR Model) has been included in the *UHIMPT* model. Nonetheless, it is noted that, if desired, the *UHIMPT* model could be reformulated to include a multiple linear regression model derived from data representing a more specific (i.e., smaller) area. In such a scenario, however, the *UHIMPT* should only be used to simulate conditions within the area that is represented by the data. Additionally, it is important to ensure that the resampled data is evenly distributed and results in a logical model; resampling the data in the manner that has been described here may result in an uneven distribution and illogical model.

In addition to the above, it is noted that the *UHIMPT* model, and specifically as represented in equations 5 and 6, includes only an adaptation of the aforementioned MLR Model. The constant of the MLR Model (31.661) has been excluded from equations 5 and 6, and has been replaced with the mean and mean maximum urban heat island amplitude of the warmest month in a given time step ($\bar{A}_{x_{Warmest\ Month}}$ and $\bar{A}_{x,Maximum_{Warmest\ Month}}$, respectively), as represented below:

**Equation 5: Modification of Mean Warmest Month Urban Heat Island Amplitude**

$$\bar{A}_{x_{Warmest\ Month,Modified}} = \bar{A}_{x_{Warmest\ Month}} + \left(\left(\frac{(\beta_i \times \Delta\bar{I}) - (\beta_v \times \Delta\bar{V}) - (\beta_\alpha \times \Delta\bar{\alpha}) - 2.82}{1.15}\right) + 2.452\right), \text{ and}$$

**Supplement B: Development of Multiple Linear Regression Model Used in Equations 5 and 6 (Continued)**

**Equation 6: Modification of Mean Maximum Warmest Month Urban Heat Island Amplitude**

$$\bar{A}_{x,Maximum_{Warmest\ Month},Modified} = \bar{A}_{x,Maximum_{Warmest\ Month}} + \left(\left(\frac{(\beta_i \times \Delta\bar{I}) - (\beta_v \times \Delta\bar{V}) - (\beta_\alpha \times \Delta\bar{\alpha}) - 2.82}{1.15}\right) + 2.452\right),$$

where: $\bar{A}$ represents mean urban heat island amplitude; $\Delta\bar{I}$ represents the change in mean proportion of impervious surface cover in the urban area; $\Delta\bar{V}$ represents the change in mean proportion of vegetation in the urban area; $\Delta\bar{\alpha}$ represents the change in mean surface albedo in the urban area; $\beta_i$ represents the standard (i.e., beta [$\beta$]) coefficient for proportion of impervious surface cover (viz., 2.103) that results when the surface albedo and proportions of impervious surface cover and vegetation of a given area are regressed on its land surface temperature; $\beta_v$ represents the standard (i.e., beta [$\beta$]) coefficient for proportion of vegetation (viz., $-8.730$) that results when the surface albedo and proportions of impervious surface cover and vegetation of a given area are regressed on its land surface temperature; $\beta_\alpha$ represents the standard (i.e., beta [$\beta$]) coefficient for surface albedo (viz., $-5.874$) that results when the surface albedo and proportions of impervious surface cover and vegetation of a given area are regressed on its land surface temperature; and, subscripts, other than those contained in predictor (i.e., beta [$\beta$]) values, specify magnitudinal (e.g., maximum), temporal (e.g.: warmest month; current time step, as specified by $x$), and other characteristics (viz., modified, which signifies that the urban heat island amplitude in a given time step is modified by the right side of the equation) such that $\bar{A}_{x,Maximum_{Warmest\ Month}}$ represents the mean maximum urban heat island amplitude of the warmest month in a given time step.

Replacement of the constant of the MLR Model with $\bar{A}_{x_{Warmest\ Month}}$ and $\bar{A}_{x,Maximum_{Warmest\ Month}}$ in equations 5 and 6 is explained by the fact that said equations are intended only for use in simulating how the modification of the proportion of impervious surface cover, the proportion of vegetation, and surface albedo impacts land surface temperature (n.b., as explained in the article, equations 5 and 6 convert land surface temperature to ambient temperature). The initial urban heat island amplitude of the time step, which fills the role of the constant in equations 5 and 6, however, is more precisely calculated by equations 3 and 4, the results of which are included in equations 5 and 6 as $\bar{A}_{x_{Warmest\ Month}}$ and $\bar{A}_{x,Maximum_{Warmest\ Month}}$. The acceptability of this adaptation of MLR Model is confirmed by the fact that the relative impacts of the independent variables remain unchanged over the original (i.e., un-adapted) form of the MLR Model.

**Supplement C: Philadelphia-Specific Data Inputs to Demonstrative *UHIMPT* Model**

| Population Inputs | | | | |
|---|---|---|---|---|
| **Age Cohort** | **2000 Population*** | **2010 Population*** | **Births**** | **Deaths**** |
| < 1 Year | 19,732 | 21,077 | 0 | 2,340 |
| 1 Year | 19,414 | 20,649 | 0 | 115 |
| 2 Years | 19,257 | 20,333 | 0 | 85 |
| 3 Years | 19,403 | 19,912 | 0 | 71 |
| 4 Years | 20,355 | 19,082 | 0 | 54 |
| 5 Years | 21,198 | 18,534 | 0 | 54 |
| 6 Years | 22,048 | 18,576 | 0 | 41 |
| 7 Years | 22,370 | 18,022 | 0 | 41 |
| 8 Years | 22,908 | 17,672 | 0 | 14 |
| 9 Years | 23,587 | 18,023 | 0 | 24 |
| 10 Years | 23,965 | 18,300 | 0 | 37 |
| 11 Years | 22,958 | 18,017 | 0 | 27 |
| 12 Years | 22,650 | 17,803 | 25 | 44 |
| 13 Years | 21,879 | 17,929 | 126 | 71 |
| 14 Years | 21,274 | 18,591 | 669 | 58 |
| 15 Years | 20,106 | 19,604 | 2,080 | 68 |
| 16 Years | 19,814 | 20,337 | 4,178 | 91 |
| 17 Years | 20,551 | 21,376 | 6,772 | 156 |
| 18 Years | 23,844 | 25,940 | 9,667 | 240 |
| 19 Years | 26,386 | 31,040 | 11,751 | 240 |

* Source: United States Census Bureau ** Source: Pennsylvania Department of Health

**Supplement C: Philadelphia-Specific Data Inputs to Demonstrative *UHIMPT* Model (Continued)**

| Population Inputs (Continued) | | | | |
|---|---|---|---|---|
| **Age Cohort** | **2000 Population*** | **2010 Population*** | **Births**** | **Deaths**** |
| 20 Years | 25,535 | 30,794 | 11,721 | 288 |
| 21 Years | 24,143 | 29,314 | 12,086 | 281 |
| 22 Years | 23,123 | 28,825 | 12,854 | 291 |
| 23 Years | 22,449 | 28,914 | 12,525 | 308 |
| 24 Years | 22,359 | 28,870 | 12,677 | 325 |
| 25 Years | 22,974 | 28,225 | 10,397 | 338 |
| 26 Years | 21,763 | 27,365 | 10,855 | 328 |
| 27 Years | 22,308 | 27,541 | 11,740 | 294 |
| 28 Years | 23,136 | 26,499 | 12,198 | 318 |
| 29 Years | 24,172 | 25,980 | 12,558 | 278 |
| 30 Years | 24,305 | 25,471 | 9,602 | 376 |
| 31 Years | 21,685 | 22,925 | 9,585 | 291 |
| 32 Years | 21,828 | 22,073 | 8,797 | 342 |
| 33 Years | 21,125 | 20,359 | 8,050 | 352 |
| 34 Years | 21,568 | 19,624 | 7,386 | 379 |
| 35 Years | 22,898 | 19,190 | 6,136 | 372 |
| 36 Years | 22,342 | 17,995 | 5,190 | 426 |
| 37 Years | 21,669 | 17,978 | 4,022 | 521 |
| 38 Years | 21,492 | 18,836 | 3,196 | 569 |
| 39 Years | 22,440 | 20,008 | 2,412 | 616 |

* Source: United States Census Bureau

** Source: Pennsylvania Department of Health

**Supplement C: Philadelphia-Specific Data Inputs to Demonstrative *UHIMPT* Model (Continued)**

| Population Inputs (Continued) | | | | |
|---|---|---|---|---|
| **Age Cohort** | **2000 Population*** | **2010 Population*** | **Births**** | **Deaths**** |
| 40 Years | 23,301 | 19,819 | 1,883 | 640 |
| 41 Years | 21,533 | 18,504 | 1,256 | 758 |
| 42 Years | 22,103 | 18,697 | 745 | 711 |
| 43 Years | 21,306 | 18,564 | 434 | 795 |
| 44 Years | 20,826 | 18,732 | 384 | 870 |
| 45 Years | 21,130 | 19,857 | 305 | 951 |
| 46 Years | 19,551 | 19,715 | 0 | 1,090 |
| 47 Years | 19,272 | 19,456 | 0 | 1,093 |
| 48 Years | 18,523 | 19,203 | 0 | 1,063 |
| 49 Years | 18,539 | 19,855 | 0 | 1,252 |
| 50 Years | 19,047 | 20,632 | 0 | 1,212 |
| 51 Years | 17,296 | 19,756 | 0 | 1,317 |
| 52 Years | 17,947 | 20,278 | 0 | 1,323 |
| 53 Years | 17,108 | 19,802 | 0 | 1,608 |
| 54 Years | 14,117 | 19,416 | 0 | 1,479 |
| 55 Years | 14,088 | 19,248 | 0 | 1,642 |
| 56 Years | 13,865 | 17,855 | 0 | 1,730 |
| 57 Years | 14,477 | 17,465 | 0 | 1,841 |
| 58 Years | 12,556 | 16,462 | 0 | 1,723 |
| 59 Years | 12,294 | 16,667 | 0 | 1,909 |

* Source: United States Census Bureau

** Source: Pennsylvania Department of Health

**Supplement C: Philadelphia-Specific Data Inputs to Demonstrative *UHIMPT* Model (Continued)**

| Population Inputs (Continued) | | | | |
|---|---|---|---|---|
| **Age Cohort** | **2000 Population*** | **2010 Population*** | **Births**** | **Deaths**** |
| 60 Years | 12,286 | 15,946 | 0 | 1,865 |
| 61 Years | 11,505 | 15,233 | 0 | 1,953 |
| 62 Years | 11,809 | 15,453 | 0 | 2,153 |
| 63 Years | 11,139 | 14,707 | 0 | 2,119 |
| 64 Years | 11,197 | 11,772 | 0 | 2,109 |
| 65 Years | 11,305 | 11,466 | 0 | 2,068 |
| 66 Years | 10,526 | 11,103 | 0 | 2,298 |
| 67 Years | 10,832 | 11,429 | 0 | 2,139 |
| 68 Years | 10,494 | 9,836 | 0 | 2,440 |
| 69 Years | 10,965 | 9,357 | 0 | 2,650 |
| 70 Years | 11,042 | 8,944 | 0 | 2,752 |
| 71 Years | 10,440 | 8,586 | 0 | 2,941 |
| 72 Years | 10,739 | 8,456 | 0 | 3,029 |
| 73 Years | 10,207 | 7,861 | 0 | 3,337 |
| 74 Years | 10,498 | 7,726 | 0 | 3,452 |
| 75 Years | 10,298 | 7,624 | 0 | 3,855 |
| 76 Years | 9,831 | 6,923 | 0 | 4,258 |
| 77 Years | 9,150 | 6,805 | 0 | 4,566 |
| 78 Years | 9,055 | 6,761 | 0 | 4,583 |
| 79 Years | 8,532 | 6,554 | 0 | 4,786 |

* Source: United States Census Bureau ** Source: Pennsylvania Department of Health

**Supplement C: Philadelphia-Specific Data Inputs to Demonstrative *UHIMPT* Model (Continued)**

| Population Inputs (Continued) | | | | |
|---|---|---|---|---|
| **Age Cohort** | **2000 Population*** | **2010 Population*** | **Births**** | **Deaths**** |
| 80 Years | 8,214 | 6,157 | 0 | 5,206 |
| 81 Years | 6,964 | 5,828 | 0 | 5,476 |
| 82 Years | 6,523 | 5,702 | 0 | 5,503 |
| 83 Years | 5,614 | 5,094 | 0 | 5,524 |
| 84 Years | 5,154 | 4,986 | 0 | 5,690 |
| 85 Years | 4,874 | 4,589 | 0 | 5,754 |
| 86 Years | 4,069 | 4,132 | 0 | 5,466 |
| 87 Years | 3,648 | 3,696 | 0 | 5,118 |
| 88 Years | 2,876 | 3,103 | 0 | 5,138 |
| 89 Years | 2,712 | 2,826 | 0 | 4,887 |
| 90 Years | 2,096 | 2,240 | 0 | 4,217 |
| 91 Years | 1,628 | 1,827 | 0 | 3,649 |
| 92 Years | 1,395 | 1,404 | 0 | 3,320 |
| 93 Years | 1,025 | 1,110 | 0 | 2,616 |
| 94 Years | 815 | 869 | 0 | 2,379 |
| 95 Years | 630 | 718 | 0 | 1,929 |
| 96 Years | 436 | 489 | 0 | 1,499 |
| 97 Years | 362 | 374 | 0 | 1,019 |
| 98 Years | 207 | 248 | 0 | 660 |
| 99 Years | 211 | 197 | 0 | 78 |
| ≥ 100 Years | 355 | 289 | 0 | 10 |

* Source: United States Census Bureau

** Source: Pennsylvania Department of Health

**Supplement C: Philadelphia-Specific Data Inputs to Demonstrative *UHIMPT* Model (Continued)**

| Climate Inputs* | | | |
|---|---|---|---|
| **Input** | **Rural** | **Urban** | **Region** |
| Last Year Represented by Climate Norm | 2010 | 2010 | 2010 |
| Normal Mean Warmest Month Temperature | 24.3358 | 25.1167 | — |
| Normal Mean Maximum Warmest Month Temperature | 30.2288 | 30.4175 | — |
| Normal Mean Annual Temperature | — | — | 12.2539 |
| Normal Mean Summer Temperature | — | — | 23.2760 |
| Normal Mean Winter Temperature | — | — | 0.9525 |
| Projected Mean Annual Temperature (Period 1) | — | — | 13.4335 |
| Projected Mean Annual Temperature (Period 2) | — | — | 15.0754 |
| Projected Mean Annual Temperature (Period 3) | — | — | 16.8857 |
| Projected Mean Warmest Month Temperature (Period 1) | 25.7293 | 26.4736 | — |
| Projected Mean Maximum Warmest Month Temperature (Period 1) | 31.7643 | 31.9823 | — |
| Projected Mean Warmest Month Temperature (Period 2) | 27.4590 | 28.2037 | — |
| Projected Mean Maximum Warmest Month Temperature (Period 2) | 33.5278 | 33.7454 | — |
| Projected Mean Warmest Month Temperature (Period 3) | 29.4353 | 30.1688 | — |
| Projected Mean Maximum Warmest Month Temperature (Period 3) | 35.5536 | 35.7608 | — |
| First Year of Projection Period 1 | 2011 | 2011 | 2011 |
| Last Year of Projection Period 1 | 2040 | 2040 | 2040 |
| First Year of Projection Period 2 | 2041 | 2041 | 2041 |
| Last Year of Projection Period 2 | 2070 | 2070 | 2070 |
| First Year of Projection Period 3 | 2071 | 2071 | 2071 |
| Last Year of Projection Period 3 | 2100 | 2100 | 2100 |

* All climate inputs obtained/derived from Wang et al. [56]

**Supplement D: Demonstrative *UHIMPT* Model in STELLA (.STMX) File Format**

The file entitled "SUPPLEMENT D (UHIMPT Model as Demonstrated in Section 3.1 of Article).stmx," which is provided in the subfolder entitled "Supporting Files," contains the *UHIMPT* model as used in the demonstration that is discussed in Section 3.1 of the article.

Please note that the file is in the STELLA (.stmx) file format and can be opened in STELLA software, which is published by isee systems, Inc. of Lebanon, New Hampshire (https://www.iseesystems.com).